


ORIGINAL ARTICLE

Beneficial effects of hepatic cyclooxygenase-2 expression against cholestatic injury after common bile duct ligation in mice

Rocío Brea¹  | Natalia Casanova¹  | Carlota Alvarez-Lucena¹  |
 Marina Fuertes-Agudo^{2,3}  | María Luque-Tevar^{2,3}  | Carme Cucarella^{2,3}  |
 María C. Capitani⁴  | María V. Marinochi⁴  | Matías E. Fusini⁵  | Agustín Lahoz⁶  |
 Marina López Noguerol⁶  | Juan Fraile¹  | María T Ronco⁴  | Lisardo Bosca^{1,7}  |
 Águeda González-Rodríguez^{1,8}  | Carmelo García-Monzón^{3,9}  |
 Paloma Martín-Sanz^{1,3}  | Marta Casado^{2,3}  | Daniel E. Francés⁴ 

¹Instituto de Investigaciones Biomédicas Sols-Morreale (IIBM), CSIC-UAM, Madrid, Spain

²Instituto de Biomedicina de Valencia (IBV), CSIC, Valencia, Spain

³Centro de Investigación Biomédica en Red de Enfermedades Hepáticas y Digestivas (CIBERehd), Madrid, Spain

⁴Instituto de Fisiología Experimental (IFISE-CONICET), Rosario, Argentina

⁵Cátedra de Histología y Embriología Humana-Fac. Cs. Médicas-UNR, Rosario, Argentina

⁶IIS-Hospital La Fe, Valencia, Spain

⁷Centro de Investigación Biomédica en Red de Enfermedades Cardiovasculares (CIBERCV), Madrid, Spain

⁸Centro de Investigación Biomédica en Red de Diabetes y Enfermedades Metabólicas Asociadas (CIBERDEM), Madrid, Spain

⁹Liver Research Unit, Hospital Universitario Santa Cristina, Instituto de Investigación Sanitaria Princesa, Madrid, Spain

Correspondence

Marta Casado, Instituto de Biomedicina de Valencia (IBV), CSIC, Jaime Roig 11, Valencia 46010, Spain.

Email: mcasado@ibv.csic.es

Daniel E. Francés, Instituto de Fisiología Experimental (IFISE-CONICET), Suipacha 570, Rosario 2000, Argentina.

Email: frances@ifise-conicet.gov.ar

Funding information

Ministerio de Ciencia e Innovación/Agencia Estatal de Investigación/10.13039/501100011033; Agencia Nacional de Promoción Científica y Tecnológica

Handling Editor: Alessio Aghemo.

Abstract

Background and Aims: Cyclooxygenase-2 (COX-2) is involved in different liver diseases, but little is known about the significance of COX-2 in cholestatic injury. This study was designed to elucidate the role of COX-2 expression in hepatocytes during the pathogenesis of obstructive cholestasis.

Methods: We used genetically modified mice constitutively expressing human COX-2 in hepatocytes. Transgenic mice (*hCOX-2-Tg*) and their wild-type (Wt) littermates were either subjected to a mid-abdominal laparotomy or common bile duct ligation (BDL) for 2 or 5 days. Then, we explored the mechanisms underlying the role of COX-2 and its derived prostaglandins in liver function, and the synthesis and excretion of bile acids (BA) in response to cholestatic liver injury.

Abbreviations: ALT, alanine transaminase; AST, aspartate transaminase; BA, bile acids; BAX, BCL-2-associated X protein; BCL-2, B-cell lymphoma 2; BDL, bile duct ligation; CA, cholic acid; CDCA, chenodeoxycholic acid; COX-2, cyclooxygenase-2; CYP7A1, cholesterol 7 α -hydroxylase; DFU, (5,5-dimethyl-3(3-fluorophenyl)-4-(4-methylsulfonyl)phenyl-2(5H)-furanone); IL-1 β , interleukin 1 β ; JNK, c-Jun N-terminal kinase; Ly6G, lymphocyte antigen 6 complex locus G; MCA, muricholic acid; MnSOD, superoxide dismutase 2; MRP3, multidrug resistance protein 3; NCL, neonatal cell line; PGE₂, prostaglandin E₂; TNF- α , tumour necrosis factor α .

Paloma Martín-Sanz, Marta Casado, and Daniel E. Francés share senior authorship.

This is an open access article under the terms of the [Creative Commons Attribution-NonCommercial-NoDerivs](https://creativecommons.org/licenses/by-nc-nd/4.0/) License, which permits use and distribution in any medium, provided the original work is properly cited, the use is non-commercial and no modifications or adaptations are made.

© 2024 The Author(s). *Liver International* published by John Wiley & Sons Ltd.

Results: After BDL, *hCOX-2-Tg* mice showed lower grades of hepatic necrosis and inflammation than *Wt* mice, in part by a reduced hepatic neutrophil recruitment associated with lower mRNA levels of pro-inflammatory cytokines. Furthermore, *hCOX-2-Tg* mice displayed a differential metabolic pattern of BA synthesis that led to an improved clearance after BDL-induced accumulation. In addition, an enhanced response to the BDL-induced oxidative stress and hepatic apoptosis was observed. In vitro experiments using hepatic cells that stably express *hCOX-2* confirmed the cytoprotective role of prostaglandin E_2 against BA toxicity.

Conclusions: Taken together, our data indicate that constitutive expression of *COX-2* in hepatocytes ameliorates cholestatic liver injury in mice by reducing inflammation and cell damage and by modulating BA metabolism, pointing to a role for *COX-2* as a defensive response against cholestasis-derived BA accumulation and injury.

KEYWORDS

BDL, bile acids, cholestasis, *COX-2*, liver, PGE_2

1 | INTRODUCTION

Cholestatic liver diseases are defined by an alteration of bile flow and are characterized by toxic retention of bile acids (BA) and other pathological features, including bile duct proliferation, proinflammatory processes, cell death, oxidative stress, and fibrosis, culminating in liver failure.¹ However, the liver has the remarkable capacity of generating an adaptive response to minimize the damage. To decrease toxicity, hepatocytes reduce the BA uptake and synthesis, transforming them into fewer toxic forms of BA, which facilitates urinary elimination.² Currently, there is no specific treatment for cholestatic diseases due to poor knowledge of their pathogenesis.³ Cholestasis-like features can be induced in rodents via surgical ligation of the common bile duct (BDL),³ which results in similar changes to those found in human cholestasis.⁴

The classic BA synthesis is initiated from cholesterol by CYP7A1 (cholesterol 7 α -hydroxylase). In humans, cholic acid (CA) and chenodeoxycholic acid (CDCA) are the primary BA synthesized in the liver.⁵ In mice, the majority of CDCA is metabolized by CYP2C70 to α -muricholic acid (α MCA) which is epimerized to β MCA. Moreover, CYP2C70 also converts ursodeoxycholic acid to β MCA.⁶ A higher degree of hydrophilicity of the BA pool allows enhanced renal clearance.⁷ After BDL, the levels of polyhydroxy-BA are markedly elevated, like several efflux pumps as a liver strategy for detoxification.⁸

Cyclooxygenases (*COX-1*, *COX-2*) are key actors in the biosynthesis of prostanoids. Through the use of a genetically modified mouse model with a constitutive expression of human *COX-2* in hepatocytes (*hCOX-2-Tg*), we have demonstrated that this *COX-2* expression protects against liver injury in several models,^{9–15} supporting a protective role of *COX-2* as a physiologic response against liver damage.

COX-2's effects on cholestasis have been controversial. Selective *COX-2* inhibitor meloxicam reduces hepatic damage

Key points

- *hCOX-2* transgenic mice have attenuated hepatic injury after bile duct ligation.
- Continuous liver prostaglandin E_2 production plays a protective role against cholestatic injury.
- Cyclooxygenase-2 (*COX-2*) enhances anti-inflammatory, anti-oxidant and anti-apoptotic responses.
- *COX-2* expression attenuates injury by modulating bile acids homeostasis.
- Pharmacological induction of *COX-2* can attenuate cholestatic injury.

caused by BDL in rats.¹⁶ However, similar short-term use of celecoxib, another selective *COX-2* inhibitor, is associated with prolonged cholestasis in humans.¹⁷ Moreover, it has recently been reported that prostaglandin E_2 (PGE_2) receptor EP4 deficiency leads to alterations in BA synthesis and plasma cholesterol levels¹⁸ by modulation of CYP7A1.¹⁹ Also, it was reported that BA induce *COX-2* in a cholangiocarcinoma cell line²⁰ and that it can inhibit 15-hydroxyprostaglandin dehydrogenase in colonocytes, leading to higher levels of PGE_2 .²¹ Apoptosis is a direct consequence of intrahepatic BA accumulation-derived injury,²² and oxidative stress is involved in this type of cell death during cholestasis. In this regard, c-Jun N-terminal kinase (JNK) is a key factor in hepatic cell death derived from obstructive cholestasis.²³ Additionally, *COX-2* expression and PGE_2 production confer cytoprotection through a decrease in pro-apoptotic proteins and the proinflammatory response,^{10,11,24} as well as through the regulation of the antioxidant response.^{11,14} All these data prompt us to elucidate the role of *COX-2* in cholestasis using *hCOX-2-Tg* mice.⁹ Our results suggest that *COX-2* plays a hepatoprotective role against cholestatic

injury by modulating inflammatory and anti-oxidative responses, cell death, BA synthesis and metabolism.

2 | MATERIALS AND METHODS

2.1 | Chemicals

The antibodies were obtained from Abcam (Cambridge, UK), Cayman (Ann Arbor, USA), Cell Signaling Technology (Danvers, USA), Santa Cruz Biotechnology (Dallas, USA), Calbiochem/Merck Millipore (Billerica, USA), and Enzo Life Sciences (Farmingdale, USA). Reagents used for Western Blot (WB) were purchased from Bio-Rad (Hercules, USA).

2.2 | Animal experimentation

Six to eight-week-old male *hCOX-2-Tg* and *Wt* sibling mice with mixed genetic backgrounds (B6D2JRccHsd) were used.⁹ Only male mice were used in procedures to avoid hormonal modulation of endogenous prostaglandin levels. Mice were kept in cycles of 12 h of light/dark in temperature (22°C) and humidity-controlled rooms, fed standard chow diet ad libitum, and with free access to drinking water. To induce cholestasis, animals were subjected to bile duct ligation (BDL) as described previously.²⁵ After surgery, all mice were given a therapeutic dose of around 60 mg/kg/day of acetaminophen (APAP) (Merck-Sigma Aldrich, St. Louis, USA) mixed in the drinking water as postoperative analgesia until euthanasia. At this dose, no modulation of COX-2 expression has been observed in rodents.²⁶ We chose two-time points post-BDL and corresponding sham-operated controls to study the effect of COX-2 expression. The selected time frames were 2 and 5 days, to evaluate its effect on acute inflammatory damage and peak of regeneration, respectively. Our prior research has shown that COX-2 has a cytoprotective effect in both scenarios.^{12,14,27} Two or five days after BDL, mice were euthanized. Blood was collected from cardiac puncture and processed for biochemical parameters. The liver was immediately frozen in liquid nitrogen and stored at -80°C or fixed with 4% paraformaldehyde (PFA) for subsequent analysis. Animal experimentation was conducted in compliance with FELASA guidelines, European Community Law (2010/63/UE), and Spanish Law (RD 53/2013). The Ethics Committee of the Bioethics Commission of the CSIC, Spain approved the research.

2.3 | Immunohistochemistry

Paraffin-embedded mice liver biopsy sections (5 µm), fixed in 4% PFA overnight at 4°C, were stained with haematoxylin and eosin, and then evaluated by a single blinded hepatohistologist (M.E.F.). For immunofluorescence, liver samples were also transferred to 10%, 20%, and 30% sucrose in PBS at 4°C until tissue sunk and embedded

in OCT. Cryosections (5 µm) were stained with anti-lymphocyte antigen 6 complex locus G (Ly6G)/6C or multidrug resistance protein 3 (MRP3)/ABCC3 antibodies (Table S1). Then, they were incubated with goat anti-rat Alexa Fluor 546 (A11081, Invitrogen (ThermoFisher Scientific, USA); 1/200) or donkey anti-rabbit Alexa Fluor 647 secondary antibody (A31573, Invitrogen; 1/200), respectively, and counterstained with DAPI (D1306, Invitrogen; 1/1000). Random fields (3 per mouse) were collected using a Leica PCS-SP5 confocal microscope and positively stained cells were analysed using ImageJ software (NIH).

2.4 | Biochemical blood and hepatic assays

The levels of total bilirubin, total cholesterol, ALT (alanine aminotransferase), and AST (aspartate aminotransferase) were measured in plasma, and total BA in urine, using specific colorimetric kits according to the manufacturer's instructions (BioSystems, Barcelona, Spain).

In addition, we performed a more exhaustive analysis of the different types of BA (total, primary, secondary, conjugated, non-conjugated and hydrophilic, α -, β -, and ω -muricholic acid) in plasma and liver tissue from *Wt* and *hCOX-2-Tg* mice. Samples were analysed at the Analytical Unit of the Instituto de Investigación Sanitaria La Fe (Valencia, Spain) using a UPLC-MRM-MS method validated according to FDA guidelines that allow the determination of 31 different BA.²⁸ All metabolomic data have been openly deposited in DIGITAL. CSIC (Casado, Marta; 2022; "Total data_BA [dataset]"; DIGITAL. CSIC; 10.20350/digitalCSIC/14755).

2.5 | Culture of hepatocyte cell lines

We used immortalized neonatal hepatocyte cell lines with (NCL-C) or without (NCL-V) human COX-2 expression.^{11,29} Cells were maintained in DMEM complete medium supplemented with 10% fetal bovine serum (FBS), in a 5% CO₂ humidified atmosphere, at 37°C. For the experiments, cells were seeded in 6-well plates (400 000 cells/well) or 96-well plates (10 000 cells/well), the FBS was withdrawn and, 2–5 h later, they were treated with chenodeoxycholic acid (CDCA 10, 100 or 250 µM prepared in EtOH) for 3 h (protein assay) or 24 h (MTT assay). In the protein assays, NCL-C cells were pre-treated with 5 µM (5,5-dimethyl-3(3-fluorophenyl)-4-(4-methylsulfonyl)phenyl-2(5H)-furanone) (DFU) for 4 h prior to FBS withdrawal, continuing the treatment for 90 min before the addition of 250 µM CDCA.

2.6 | MTT (thiazol blue tetrazolium blue) assay

NCL-V and NCL-C cells were seeded in 96-well plates (10 000 cells/well). After adding CDCA for 24 h, cells were washed with PBS and 100 µL of complete medium were added. After incubation, 20 µL of

MTT solution (2 mg/mL) was added to the cells, which were then incubated for 3 h at 37°C in the dark. Finally, 100 µL of DMSO were added, and the absorbance was measured at 570 and 630 nm.

2.7 | RNA extraction and quantitative polymerase chain reaction analysis

Total RNA from liver samples was extracted using TRIzol reagent (ThermoFisher Scientific) according to the manufacturer's instructions. RNA (250 ng) was reverse transcribed with the High Capacity cDNA Reverse Transcription Kit. Quantitative PCR (qPCR) was performed using 5 or 50 ng of cDNA, Power SYBR Green Master Mix, and specific primers (Table S2). Amplification was conducted in a 7900HT Fast-Real Time PCR System (Life Technologies/ThermoFisher). The PCR cycles included an initial denaturation for 10 min at 95°C, followed by 40 cycles of 15 s at 95°C and 1 min at 60°C. A dissociation curve was performed to confirm the specificity of the PCR products, consisting of 15 s at 95°C, 15 s at 60°C, and 15 s at 95°C. Data analysis is based on the $2^{-\Delta\Delta C_t}$ method with normalization of the raw data to the housekeeping gene hypoxanthine phosphoribosyl transferase 1 (*Hprt1*). Each sample was analysed in triplicate.

2.8 | Homogenization and preparation of tissue extracts and western blotting

Liver tissue and NCL cells were homogenized in ice-cold lysis buffer containing .5% CHAPS, 10 mM Tris-HCl; pH 7.5, 1 mM MgCl₂, 1 mM EDTA, 10% glycerol and protease and phosphatase inhibitors (5726, P0044, P8340, Merck-Sigma Aldrich) and cleared by centrifugation. Protein determination was performed by the Bradford dye method. Cytosolic and nuclear extracts were prepared as previously described.¹²

Protein extracts (14–30 µg) were boiled with Laemmli buffer and then separated by 8%–12% SDS-PAGE. Proteins were transferred to a polyvinylidene fluoride membrane (PVDF), blocked using 5% non-fat dried milk in PBS, and then incubated with primary antibodies (Table S1) overnight at 4°C. Then, membranes were incubated with the corresponding peroxidase-conjugated secondary antibodies for 1 h at RT. Immunoreactive bands were visualized using the ImageQuant LAS 500 (GE Healthcare Bio-Sciences, Uppsala, Sweden). The densitometric analysis was carried out with the ImageJ software.

2.9 | Data analysis

Statistical analysis was performed using one-way ANOVA followed by Fisher's LSD post hoc test, Kruskal–Wallis or *t*-Student test, as appropriate. The results were expressed as the mean ± standard error (S.E.M.) of at least four–six animals/three independent experiments.

The software used was InfoStat v2017.1.2, with $p < .05$ as the level of significance.

3 | RESULTS

3.1 | Constitutive hepatic COX-2 expression in hCOX-2-Tg mice protects against BDL-associated cholestatic damage

To investigate the impact of COX-2 expression on BDL-associated cholestatic damage, we utilized our previously described transgenic hCOX-2-Tg mouse model (Figure 1).¹² Wt mice showed extensive liver cell necrosis with chromatin condensation, organelle swelling, and cell membrane disruption at 2 and 5 days after BDL. This was significantly reduced in hCOX-2-Tg mice (as shown in Figure 1A) and confirmed by necrosis extent quantification (Figure 1B). According to the histological analysis, ALT levels were significantly elevated due to BDL intervention. However, in hCOX-2-Tg mice, ALT levels were markedly lower after 5 days of BDL (Figure 1C). In addition, these animals showed a tendency to decrease the accumulation of total bilirubin (Figure 1D). Overall, these data suggest the existence of effective cell defence mechanisms in hCOX-2-Tg mice against cholestatic damage. Moreover, after BDL, we found no differences in liver/body weight ratio between genotypes, or in human COX-2 protein expression levels in the transgenic mice (Figure S1).

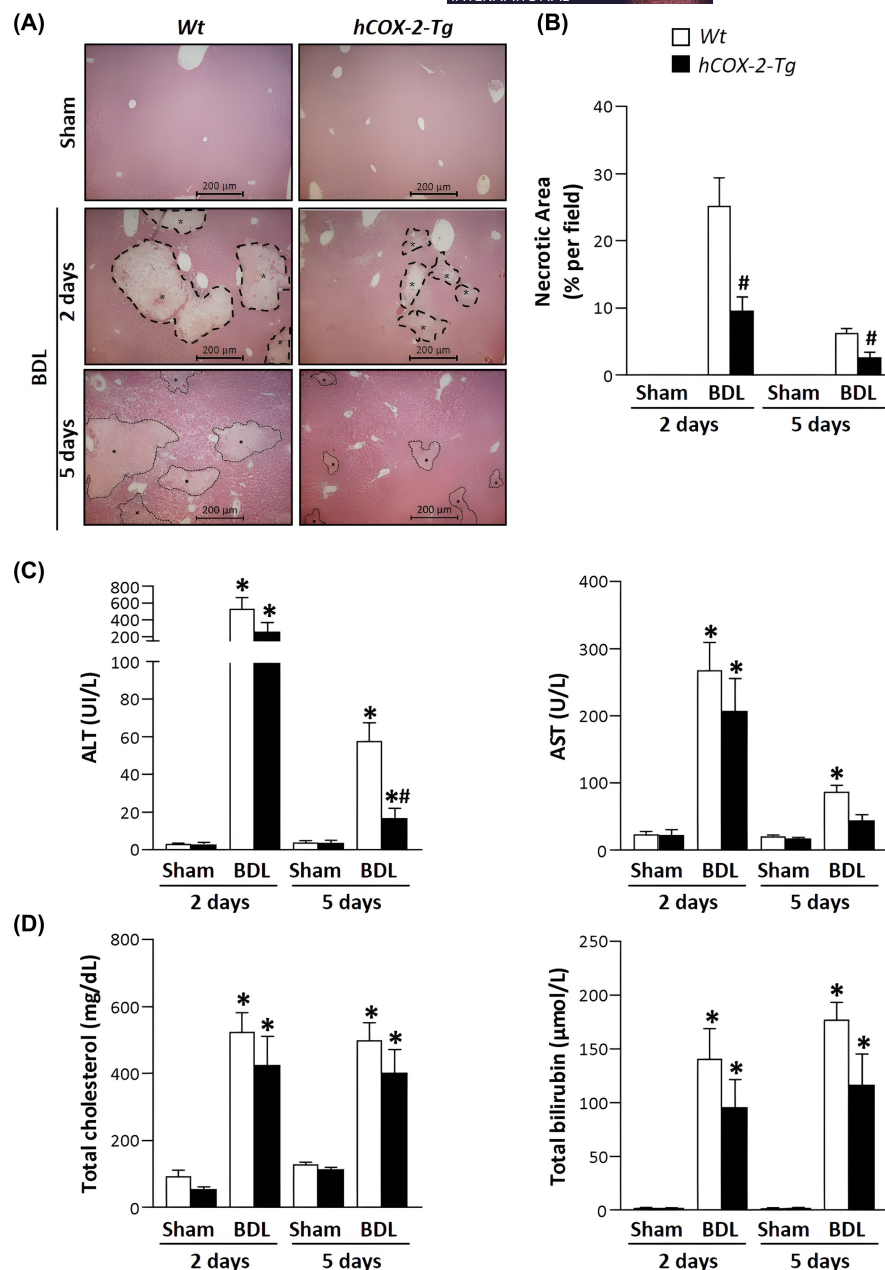
3.2 | The inflammatory injury induced by BDL is attenuated by hepatic constitutive expression of COX-2 in mice

Hepatocellular necrosis derived from BDL is accompanied by an intense inflammatory response.³⁰ Figure 2 shows the protective effect that the constitutive expression of COX-2 exhibits against the BDL-elicited inflammatory response. In this regard, Figure 2A details hepatic mRNA levels of proinflammatory cytokines involved in hepatocellular injury, such as tumour necrosis factor α (TNF- α), interleukin 6 and interleukin 1 β (IL-1 β). Constitutive COX-2 expression seems to attenuate the increase of mRNA levels found 2 days post-BDL. Consistently, higher mRNA levels of *Adgre1* (encoding for F4/80), a macrophage/monocyte surface marker, were found in Wt mice 5 days post-BDL compared to hCOX-2-Tg mice.

The nuclear factor- κ B (NF κ B) signalling pathway is a key component in the progression of cholestatic injury.³⁰ We found an important increase in nuclear p65 localization in Wt BDL mice, suggesting a strong NF κ B pathway activation, while this effect was suppressed in hCOX-2-Tg mice (Figure 2B).

Additionally, at the earlier time point post-BDL (2 days), the immunofluorescence and confocal microscopy analysis showed higher levels of infiltrating lymphocyte antigen 6 complex locus G-positive (Ly6G⁺) cells (a neutrophil plasma membrane biomarker) in Wt mice when compared to hCOX-2-Tg mice (Figure 2C).

FIGURE 1 *hCOX-2-Tg* mice are protected against cholestatic-induced liver damage after BDL. (A) Representative images of H&E staining performed on sections of livers from *Wt* and *hCOX-2-Tg* mice, after Sham and 2 or 5 days after BDL surgery. (B) Necrotic area per field (expressed in %) (C) Plasmatic ALT and AST levels (expressed in international units per litre, U/L) in all experimental groups. (D) Total plasmatic cholesterol (expressed in mg/dL) and bilirubin levels (expressed in $\mu\text{mol/L}$) from *Wt* and *hCOX-2-Tg* mice, after Sham and 2 or 5 days after BDL surgery. Data are represented as the mean \pm S.E.M. ($n=4-6$ mice per group). * $p<.05$ versus *Wt* Sham; # $p<.05$ versus *Wt* BDL. BDL, bile duct ligation; H&E, hematoxylin and eosin.



3.3 | COX-2 expression attenuated hepatic cholestatic damage by an enhancement of the antioxidant, cell survival, and regenerative response

It is well known that alterations of anti-oxidant defences occur in cholestatic liver diseases.³⁰ As shown in Figure 3A, *hCOX-2-Tg* mice showed an enhanced anti-oxidant response against cholestatic damage. In this regard, Western blot analysis shows that at 5 days post-BDL there is an increased level of protein expression of superoxide dismutase 2 (MnSOD) and catalase in *hCOX-2-Tg* mice livers when compared to *Wt* counterparts.

BA-induced toxicity mechanisms involve not only oxidative stress but also endoplasmic reticulum (ER) stress.³¹ In this regard, we found that *Ddit3* (encoding for C/EBP homologous protein) was

significantly affected only in *Wt* mice 2 days post-BDL, whereas *Hspa5* (encoding for glucose-regulated protein 78) showed no modifications (Figure S2).

Protein expression levels of some important mediators of the cellular death/proliferation balance were analysed 5 days post-BDL, which corresponds to the peak of the hepatic regenerative response.¹ In our model, an attenuated activation of the JNK pathway (Figure 3B) and a lower level of the BCL-2-associated X protein (BAX/BCL-2) ratio (Figure 3C) were found in *hCOX-2-Tg* mice after BDL, suggesting a better anti-apoptotic response in these livers against cholestatic injury. In line with this, *hCOX-2-Tg* mice showed an enhanced regenerative and cytoprotective response, evidenced by higher activation of the AKT pathway (Figure 3D). It was demonstrated that treatments that attenuated BDL-associated liver injury

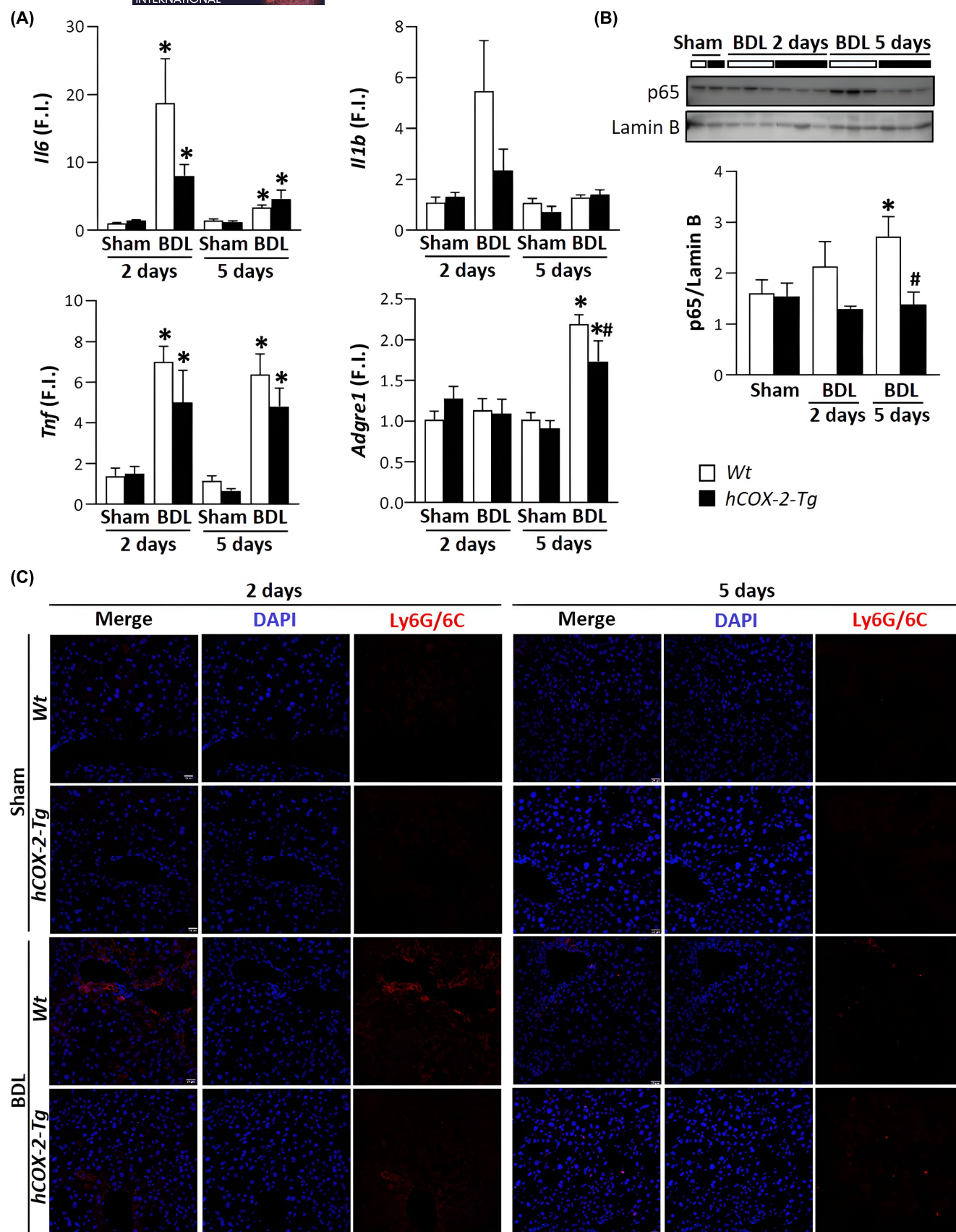
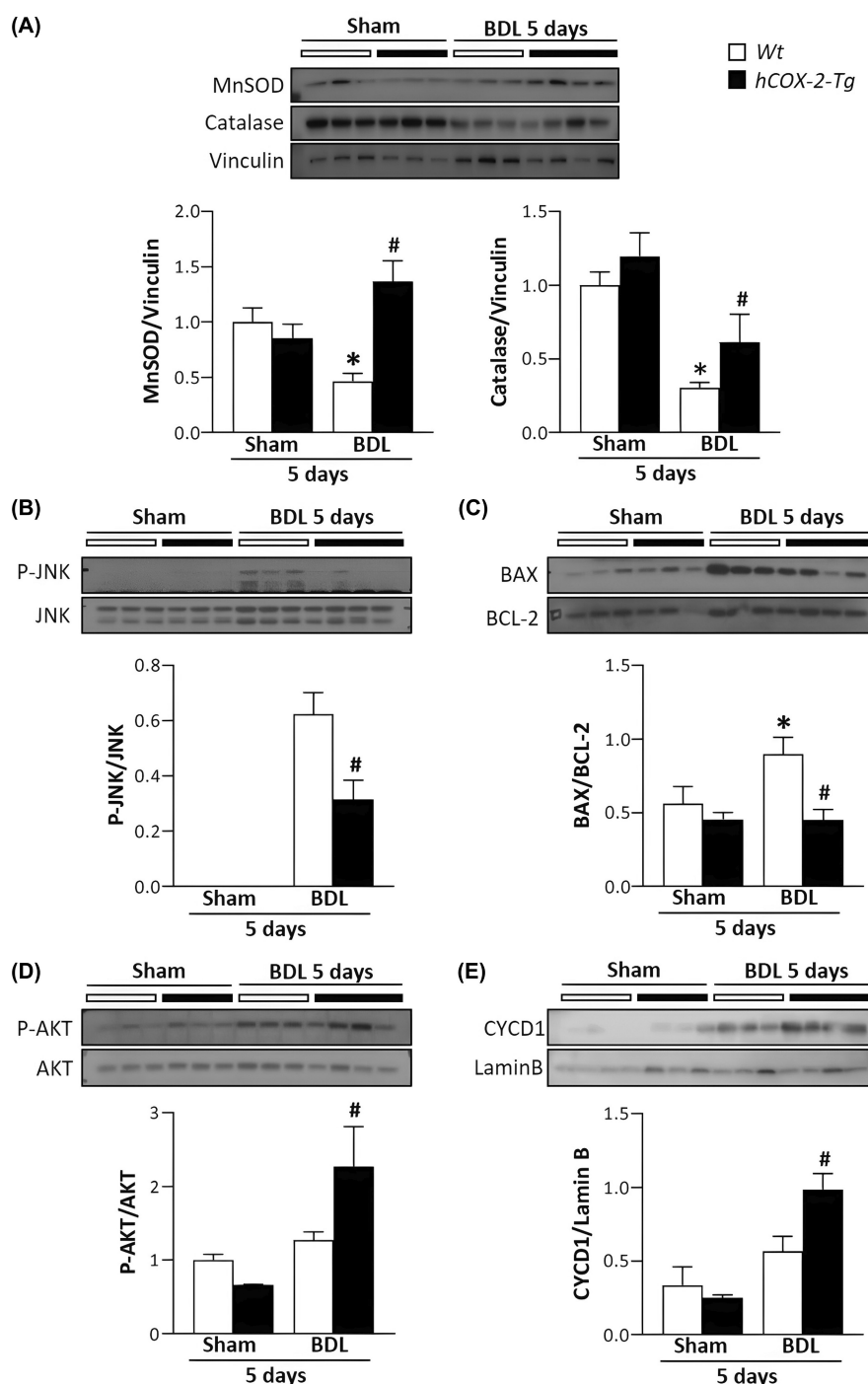


FIGURE 2 *hCOX-2-Tg* mice showed an attenuated inflammatory response after BDL. The data analysed is from *Wt* and *hCOX-2-Tg* mice, after Sham and 2 or 5 days post-BDL. (A) Liver mRNA expression of *Il6* (encoding for IL-6), *Il1b* (encoding for IL-1 β), *Tnf* (encoding for TNF- α) and *Adgre1* (encoding for F4/80) was analysed by RT-qPCR. Values have been normalized with *Hprt1* mRNA, and expressed as fold increase (F.I.) versus *Wt* Sham ($n=4-6$ mice per group). (B) Representative Western blots showing nuclear p65 protein levels in nuclear liver extracts. Lamin B levels were used as loading control ($n=4-6$ mice per group). The graph depicts densitometric quantifications of the indicated protein levels. (C) Representative images of anti-Ly6G/6C staining performed on various liver cryosections. Data are represented as the mean \pm S.E.M. * $p < .05$ versus *Wt* Sham; # $p < .05$ versus *Wt* BDL. BDL, bile duct ligation.

FIGURE 3 *hCOX-2-Tg* mice showed enhanced anti-oxidative, anti-apoptotic and proliferative responses against BDL-induced liver injury. The data analysed is from *Wt* and *hCOX-2-Tg* mice, after Sham and 5 days post-BDL. (A-E) Representative Western blots showing MnSOD, Catalase (A), P-JNK/JNK (B), BAX, BCL-2 (C), P-AKT/AKT (D) and nuclear CYCD1 (E) protein levels in liver extracts. Their respective total protein, BCL-2, vinculin or lamin B levels were used as loading control. The graphs depict densitometric quantification of the indicated protein levels. Data are represented as the mean \pm S.E.M. ($n=4-6$ mice per group) * $p < .05$ versus *Wt* Sham; # $p < .05$ versus *Wt* BDL. BDL, bile duct ligation.



enhanced hepatocyte proliferation, with upregulation of genes such as cyclin D1.³² In our model, at 5 days post-BDL we found a higher nuclear level of cyclin D1 in *hCOX-2-Tg* mice (Figure 3E) suggesting a more accelerated tissue regeneration in the livers of these animals.

These data are consistent with the histological analysis that found a considerable increase of mitotic figures only in the hepatic parenchyma of *hCOX-2-Tg* mice (Figure S3) and suggested effective defence mechanisms.

3.4 | COX-2 expression is involved in the modulation of the synthesis of different bile acids (BA)

We set out to analyse the effect of the hepatic constitutive expression of COX-2 on BA synthesis (Figure 4). For this purpose, we quantitatively measured plasmatic and hepatic levels of several BA by UPLC-MS analysis. Hepatic and plasmatic levels of primary and secondary BA found post-BDL were higher compared to sham conditions, confirming the establishment of the model.⁷ *hCOX-2-Tg* mice

showed lower total BA levels in plasma at 5 days post-BDL (Figure 4A), and in the hepatic tissue at 2 and 5-days post-BDL (Figure 4B). The analysis of the amounts of primary and secondary BA in liver samples revealed that increased toxic accumulation of BA occurring in Wt mice is preponderantly due to increased levels of primary ones (Figure 4C). Likewise, we found no differences in the levels of secondary BA between Wt and *hCOX-2-Tg* groups after BDL (Figure 4C). This prompted us to analyse *Cyp7a1* mRNA and protein levels 5 days after BDL. We found increased *Cyp7a1* mRNA levels of Wt mice post-BDL

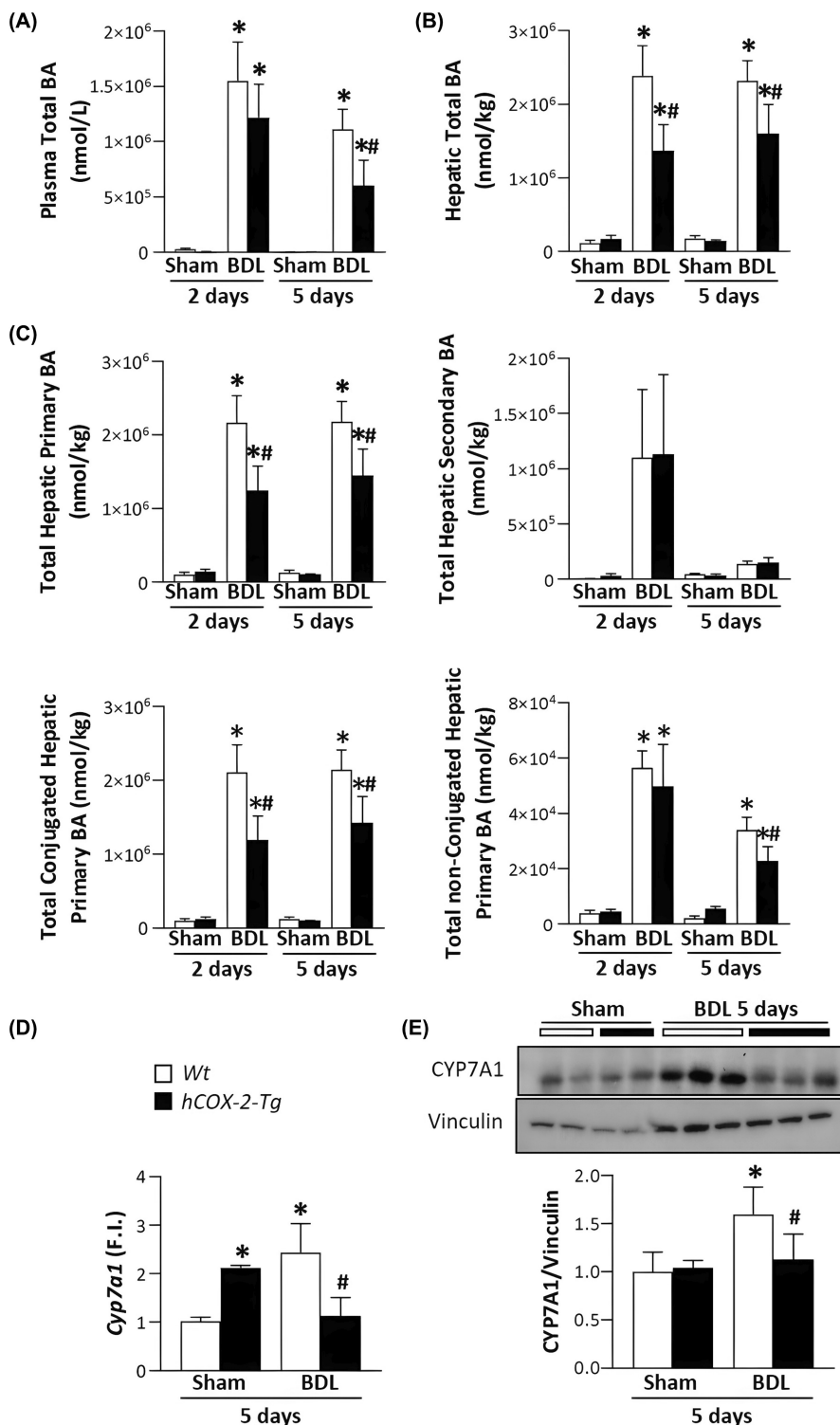


FIGURE 4 Total bile acids levels in Wt and *hCOX-2-Tg* mice, after Sham and 2 or 5 days after BDL surgery. Levels of bile acids (BA) quantified by UPLC and MS analysis. Plasma (A) and hepatic (B) levels of total BA, expressed in nmol/L (A) or nmol/kg (B). (C) Total hepatic levels of primary, secondary, conjugated and non-conjugated BA, expressed in nmol/kg. (D) Liver mRNA expression of *Cyp7a1* was analysed by RT-qPCR. Values have been normalized with *Hprt1* mRNA, and expressed as fold increase (F.I.) versus Wt Sham. (E) Representative Western blots showing CYP7A1 protein levels in liver extracts. Vinculin levels were used as loading control. The graph depicts densitometric quantifications of the indicated protein levels. Data are represented as the mean \pm S.E.M. ($n=4-6$ mice per group). * $p < .05$ versus Wt Sham; # $p < .05$ versus Wt BDL. BDL, bile duct ligation.

(Figure 4D), which explains the increased levels of primary BA by an enhanced synthesis from cholesterol. In *hCOX-2-Tg* animals, this induction was attenuated, helping to maintain the lower hepatic levels of toxic BA found in this group. The analysis of CYP7A1 protein levels (Figure 4E) confirmed the profile found in the mRNA levels. In line with this data, only in *Wt* livers, mRNA levels of *Fxr*, *Fgfr4* (negative regulators of *Cyp7a1*), and *Bsep* (*Fxr* direct target gene) were diminished after BDL, confirming the above-mentioned observations (Figure S4).

3.5 | The constitutive hepatic expression of COX-2 promotes the formation of more hydrophilic bile salts

Considering the significance of BA's hydrophilicity in the context of obstructive cholestasis, we have examined the content of more hydrophilic bile salts (Figure 5). In this regard, we found that *hCOX-2-Tg* mice showed a greater amount of more hydrophilic BA (α MCA and β MCA) in plasma after BDL (Figure 5A). Likewise, the levels of these BA increased significantly in liver samples after BDL in both genotypes, but *Wt* mice showed higher levels after 5 days, contributing to the high levels of accumulated BA observed in this genotype (Figure 5B). In this sense, higher levels of these BA in the plasma of *hCOX-2-Tg* mice post-BDL is consistent with an improved hepatic clearance of these BA in this genotype. In line with this, and after BDL, we found a decrease of *Cyp2a70* mRNA levels (essential in the biosynthesis of α MCA, β MCA) only in *Wt* mice while this drop was found attenuated in the livers of *hCOX-2-Tg* animals (Figure 5C).

3.6 | Constitutive COX-2 expression enhances the induction of the basolateral transporter MRP3 after BDL

Under cholestatic conditions, the cellular defensive response involves the induction of several ATP-dependent export pumps located in the basolateral membrane as MRP3. In our model (Figure 6), we found that after 5 days post-BDL, *Abcc3* gene expression (encoding for MRP3) was induced in both genotypes (Figure 6A), but only in *hCOX-2-Tg* animals, the protein expression was significantly increased (Figure 6B). Confocal microscopy analysis (Figure 6C) confirmed basolateral membrane localization. In addition, it was observed that transgenic animals had notably higher levels of urinary BA as compared to *Wt* BDL mice (Figure S5). This, along with the increase in MRP3 content in the basolateral membrane, indicates that the lower levels of BA found in the plasma and liver of transgenic animals after BDL are partly due to improved renal clearance.

3.7 | COX-2 expression in NCL cells protects from damage caused by the accumulation of CDCA

We next investigated whether COX-2 could protect hepatocytes from BA toxicity in vitro (Figure 7). We tested the effect of CDCA

treatment on a neonatal hepatocyte immortalized line expressing *hCOX-2* (NCL-C) vs control line (NCL-V)^{11,29} NCL cell lines were treated with CDCA at sub-cytotoxic (10 and 100 μ M) concentrations. We found that 100 μ M CDCA treatment for 24h reduced the viability of NCL-V cells significantly compared to the NCL-C cells (Figure 7A). To analyse the pathways involved in this effect, cells were treated with cytotoxic concentrations of CDCA (250 μ M) for 3h. As shown in Figure 7B, the presence of *hCOX-2* prevents the increase in cleaved caspase 3 and JNK activation observed in NCL-V cells after CDCA treatment. Furthermore, when we use a specific COX-2 inhibitor, DFU, this protection against apoptosis seems to be attenuated. These data suggest that COX-2 expression and activity protect hepatocytes from damage caused by CDCA accumulation.

4 | DISCUSSION

During the cholestatic process, hepatic accumulation of BA inevitably leads to cell death. However, the liver has an extraordinary regenerative capacity aimed at restoring parenchymal damage and, during a cholestatic injury, several adaptive mechanisms are activated in an attempt to attenuate BA accumulation and protect hepatocytes from damage. This aim is mainly achieved by modulating BA synthesis and inducing basolateral export pumps that allow urinary excretion as an alternative route of clearance.³³ We used our *hCOX-2-Tg* transgenic mouse model with a hepatic-specific COX-2 constitutive expression to study its role in a cholestatic context. Our data reveal that *hCOX-2-Tg* mice were significantly less susceptible to cholestatic injury, as evidenced by reduced ALT levels and necrosis grade after BDL.

The inflammatory response bears a main role in the pathogenesis of several human diseases, and NF- κ B-mediated inflammatory response has been associated with several animal models of cholestasis, including BDL.³⁰ The constitutive expression of COX-2 was able to attenuate the increase of pro-inflammatory cytokines and NF- κ B activity. Also, *hCOX-2-Tg* livers presented lower levels of macrophage markers and diminished neutrophil infiltration after BDL, contributing to ameliorate cholestatic-derived cell damage. These data are in line with previous work, where lower levels of inflammatory markers and reduced hepatic leukocyte recruitment and infiltration were found in *hCOX-2-Tg* mice upon hepatic injury derived from different insults.^{12,14,24}

Chronic liver injury that follows BDL is characterized by an increase in the hepatic oxidative damage that has been detected in obstructive cholestasis both in rodents and humans.^{34,35} It has been largely demonstrated that anti-oxidant response activation has a beneficial role in cholestatic liver injury.³⁶⁻³⁸ As other authors reported,³⁹ we found a significant decrease in MnSOD and catalase expression levels in *Wt* mice, but conversely, *hCOX-2-Tg* livers are more resistant to BDL-associated oxidative stress, in part, by an increased expression of these enzymes.¹⁴

In cholestasis, dead liver cells are usually present in a necrotic form, but it was reported that malfunctioning programmed

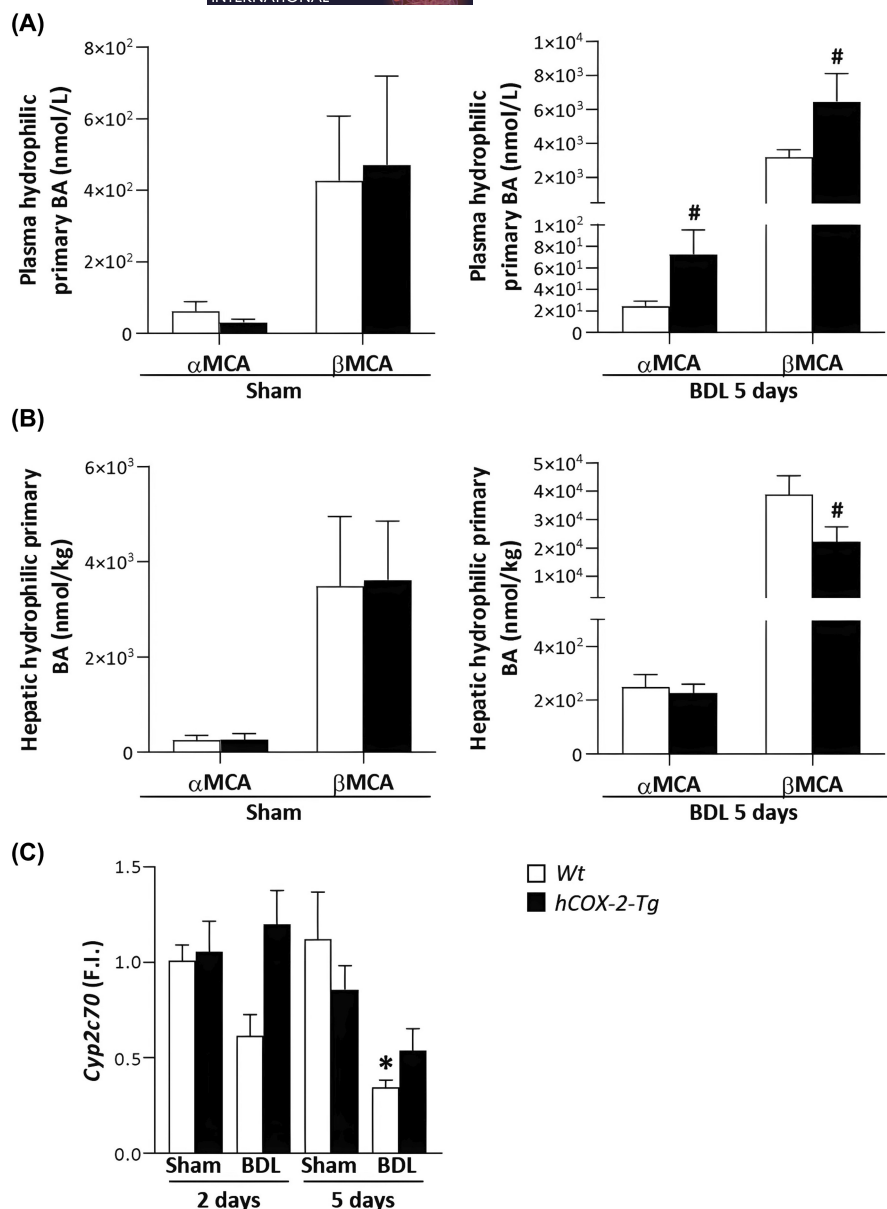


FIGURE 5 Hydrophilic muricholic acids (α MCA and β MCA) plasmatic levels are enhanced in hCOX-2-Tg livers 5 days post-BDL surgery. The data analysed is from Wt and hCOX-2-Tg mice, after Sham and 5 days after BDL surgery. (A) Concentration of the hydrophilic bile acids (BA) α MCA and β MCA in plasma (expressed in nmol/L). (B) The concentration of α MCA and β MCA in liver tissue (expressed in nmol/kg). (C) Liver mRNA expression of *Cyp2c70* analysed by RT-qPCR, values have been normalized with *Hprt1* mRNA, and expressed as fold increase (F.I.) versus Wt Sham. Data are represented as the mean \pm S.E.M. ($n=4-6$ mice per group) * $p < .05$ versus Wt Sham; # $p < .05$ versus Wt BDL. BDL, bile duct ligation.

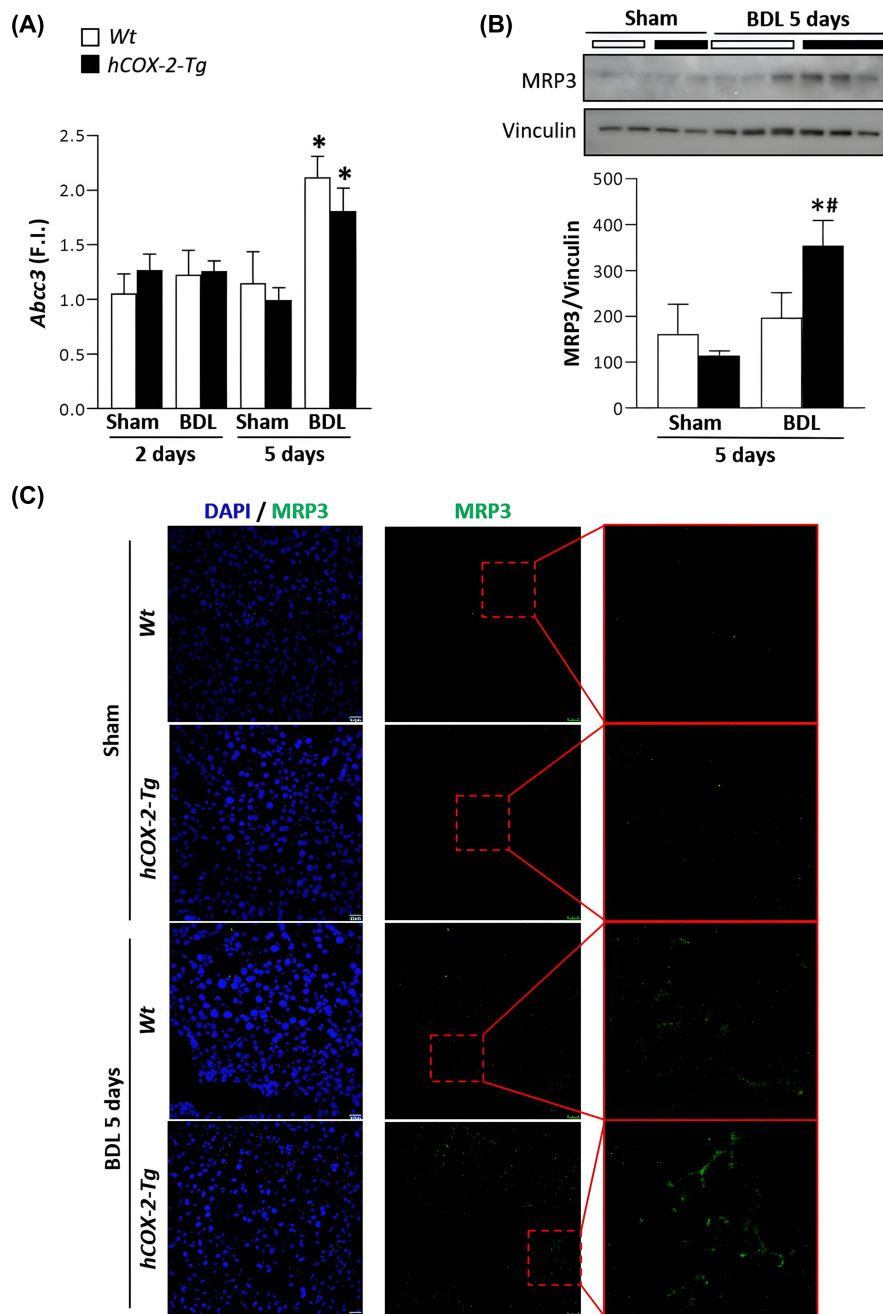
cell death is another hallmark of the disease.⁴⁰ In this regard, neutrophil-derived reactive oxygen species leads to mitochondrial dysfunction, activation of MAP kinases and apoptosis.¹ We proved that COX-2 expression reduces cholestasis-induced liver injury by blunting JNK activation. Also, the attenuated BAX/BCL-2 ratio found in hCOX-2-Tg mice after BDL, agrees with this reported effect of COX-2 induction against hepatic insult.^{9,11,14} In line with these data, we performed in vitro experiments which demonstrated that COX-2 enzymatic activity specifically prevented P-JNK activation and caspase-3 cleavage, pointing out its role against BA-induced apoptosis.

On the other hand, it is well known that after BDL, the consequent hepatocellular injury leads to gene activation and the initiation of the regenerative response with a hepatocellular proliferation peak 5 days post-surgery.² COX-2 has a key role in hepatocyte proliferation after partial hepatectomy²⁷ or several other types of hepatic injuries.^{9,24} Here, we found that hCOX-2-Tg mice not only

have an attenuated activation of pro-apoptotic pathways but also an enhanced cell survival/proliferation response against cholestatic damage. It is known that the AKT pathway is a target of PGs.⁴¹ AKT phosphorylation is enhanced in hCOX-2-Tg mice liver post-BDL, thus indicating a reinforcement of survival pathways as was described by us and others in several models of liver damage.^{10,11,24,41,42} Additionally, an enhanced proliferative response to BDL is reached by COX-2 expression, mainly by inducing cyclin D1 nuclear levels, as seen in physiological²⁷ and metabolic liver stress.¹¹

In rodents, there is a paradoxical stimulation of CYP7A1 post-BDL, and the consequent primary BA synthesis and accumulation.⁴³ We found that hepatic *Cyp7a1* mRNA level and protein expression were increased by BDL in Wt mice, and that those levels are significantly lower when COX-2 was constitutively expressed. This attenuated response was confirmed through the analysis of the negative regulators of *Cyp7a1* *Fxr*, *Bsep* or *Fgfr4*. Interestingly, this protective effect afforded by modulation against BDL-induced expression

FIGURE 6 Hepatic COX-2 expression induces MRP3 protein levels and basolateral localization after BDL. The data analysed is from Wt and *hCOX-2-Tg* mice, after Sham and 2 or 5 days after BDL surgery. (A) Liver mRNA expression of *Abcc3* (encoding for MRP3) was analysed by RT-qPCR. Values have been normalized against *Hprt1* mRNA, and expressed as fold increase (F.I.) versus Wt Sham. (B) Representative Western blots showing MRP3 protein levels in liver extracts. Vinculin levels were used as loading control. The graph depicts the quantification of the indicated protein levels. (C) Representative images of anti-MRP3 staining performed on various livers cryosections showing basolateral localization. Data are represented as the mean \pm S.E.M. ($n=4-6$ mice per group) * $p < .05$ versus Wt Sham; # $p < .05$ versus Wt BDL. BDL, bile duct ligation; COX-2, cyclooxygenase-2.



of *Cyp7a1* seems to be a common mechanism of other protective agents.³⁷

After BDL, and as a compensatory response, BA became more hydrophilic in mice livers, mainly because of increased 6 β -hydroxylation catalysed by CYP2A70.⁷ After BDL, *hCOX-2-Tg* mice showed a less cytotoxic BA pool and a concomitant improvement in clearance due to increased hydrophilicity are achieved in the face of BDL injury. Interestingly, and in concordance with our data, a previous report showed that CYP2C70 was decreased in male mice liver when treated with ibuprofen, a COX inhibitor,⁴⁴ suggesting a COX-2-dependent modulation of this pathway.

During cholestasis, MRP3 expression is markedly increased as a protective response against hepatic BA accumulation.³³ Indeed, we observed a remarkable increase in hepatic tissue levels from

hCOX-2-Tg animals. As far as we know, this is the first report that links COX-2 expression with MRP3 induction and acceleration of BA excretion during cholestasis. Accordingly, there is evidence that the induction of MRP3 depends on the anti-oxidative response,⁸ and indeed we know that the latter depends on the induction of COX-2 and its derived prostanoids in different models of liver damage.^{14,45}

Taken together, our data clearly show that constitutive COX-2 expression in the hepatocyte attenuates BDL-derived cell injury via multiple mechanisms (summarized in Figure 8), as previously described in several models of liver insults.^{10,11,14,24,27} In the presence of COX-2, there is a protective effect that is afforded in several ways: through the production of hepatoprotective prostanoids,⁹ promoting tissue regeneration,⁴⁶ by regulation of proinflammatory

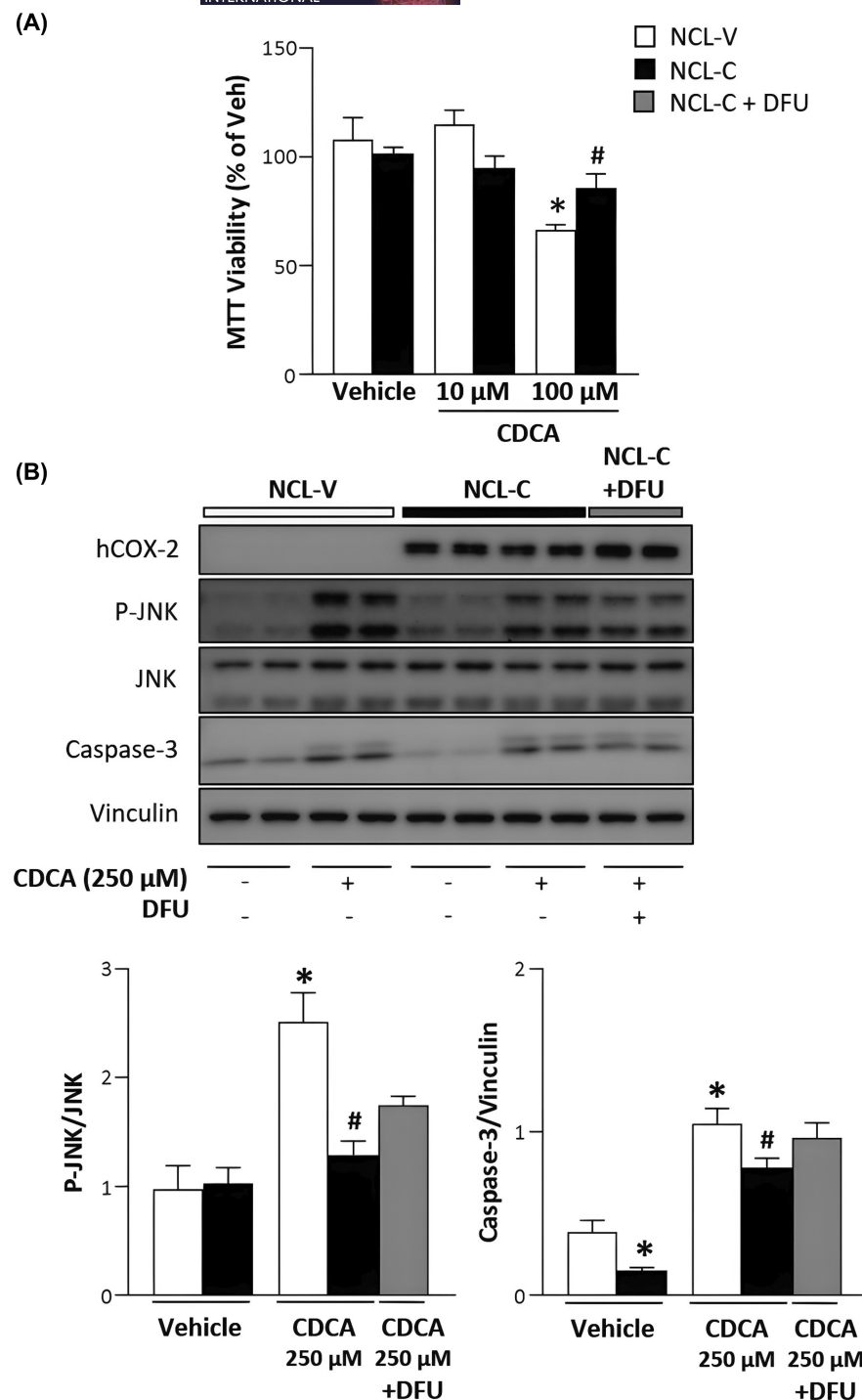


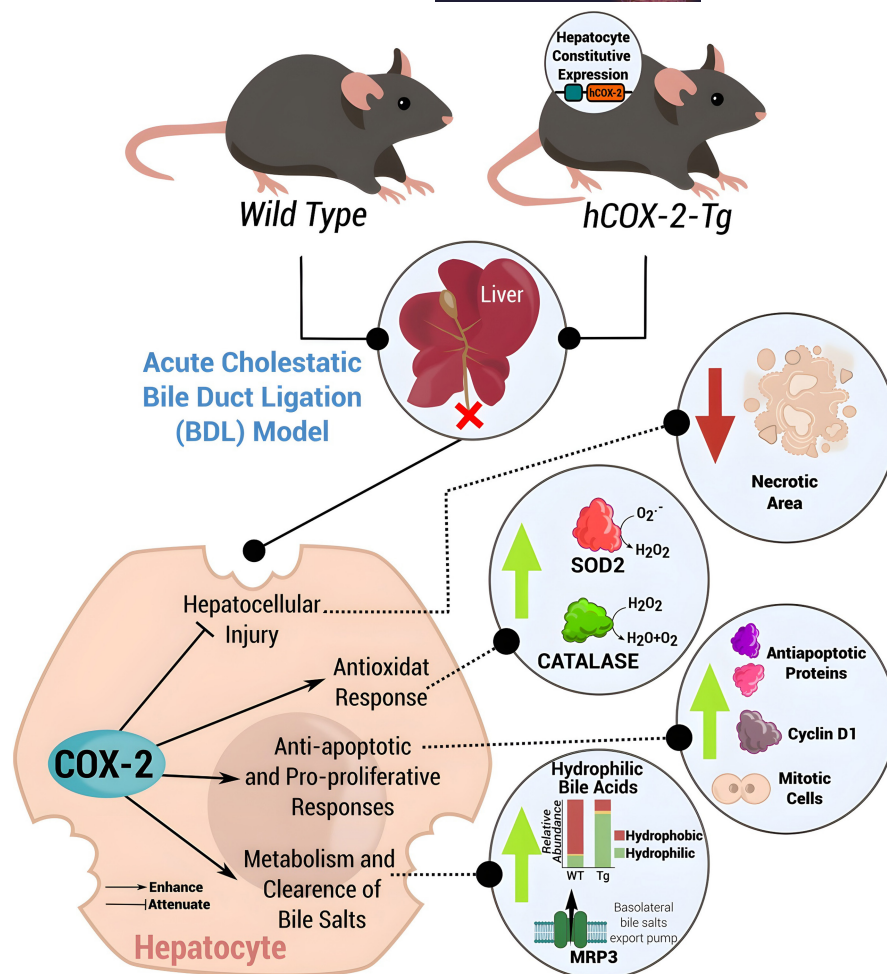
FIGURE 7 Constitutive COX-2 expression protects against BA-mediated toxicity in immortalized hepatocyte lines. (A) Cell viability after BA-treatment was assessed by MTT assay. Immortalized cell lines NCL-V and NCL-C were treated with chenodeoxycholic acid at sub-cytotoxic concentrations (CDCA 10, 100 µM prepared in EtOH) for 24 h. (B) Apoptotic cell death was measured by cleaved caspase-3 levels and JNK activation by Western blotting after 3 h of CDCA treatment (250 µM). NCL-C cells were pre-incubated for 5 h with 5 µM of specific COX-2 inhibitor DFU before CDCA treatment (NCL-C + DFU). Their respective total protein or vinculin levels were used as loading control. The graphs depict densitometric quantification of the indicated protein levels. Data are represented as the mean \pm S.E.M. ($n=3$ independent experiments). * $p < .05$ versus NCL-V Vehicle; # $p < .05$ versus NCL-V CDCA. BA, bile acids; BDL, bile duct ligation; CDCA, chenodeoxycholic acid; COX-2, cyclooxygenase-2.

cytokines, which aids in tissue recovery by driving resolution of inflammation, and enhancing a pro-survival and anti-oxidant response against injury.^{12,14} Moreover, we showed that *hCOX-2-Tg* mice have a differential metabolism of BA, enhancing hydrophilic BA production and hepatic extrusion by induction of basolateral transporters expression.

Based on a transgenic approach, we propose that the induction of COX-2 expression observed in cholestatic diseases⁴⁷ or post-BDL,¹⁶ acts as a physiological defensive response. BDL surgery has been found to provide protection against damage and induce a variety of factors post-surgery. Studies have shown that BDL inhibits

TNF- α -induced hepatocyte apoptosis by activating the AKT pathway.⁴⁸ Additionally, mice who underwent BDL showed considerable protection against ischemic liver injury by attenuating neutrophil infiltration and NF- κ B activation.⁴⁹ The defence mechanisms activated through AKT and NF κ B pathways in these circumstances are similar to those dependent on COX-2 induction.^{14,24} Our results shed new insights into a possible protective mechanism of COX-2 induction against cholestatic injury. In fact, recently it has been suggested the therapeutic use of TNF- α /IL-1 β -licensed human adipose tissue-derived stem cells that attenuate cholestatic liver injury by upregulating COX-2 expression and PGE₂ production.⁵⁰ Herein, our

FIGURE 8 Diagram outlining the key findings highlighting how the constitutive expression of COX-2 offers protection against liver injury induced by BDL. COX-2 expression in liver cells can reduce BDL-related injury through several mechanisms. COX-2 produces protective prostaglandins, promotes tissue regeneration, regulates pro-inflammatory cytokines, and enhances anti-oxidant responses. Overexpression of hCOX-2 alters bile acid metabolism, leading to increased production of hydrophilic bile acids and their elimination from the liver through transporter induction. BDL, bile duct ligation; COX-2, cyclooxygenase-2.



pre-clinical study is expected to provide new targets for cholestasis treatment by inducing COX-2 or using its products. Additionally, it will suggest prevention strategies to avoid the frequent use of COX-2 inhibitor anti-inflammatory drugs in these patients.

ACKNOWLEDGEMENTS

We appreciate Tania Dávila-Ortiz's technical assistance in manuscript revision.

FUNDING INFORMATION

This work was supported by the following projects: Ministerio de Ciencia e Innovación/Agencia Estatal de Investigación 10.13039/501100011033 (PID2022-143192OB-I00; PID2020-113238RB-I00), Research Grant PICT 2018-01446 and 2021-0152 from Agencia Nacional de Promoción Científica y Tecnológica (ANPCyT), iCOOP from CSIC (COOPB23081), Centro de Investigación Biomédica en Red en Enfermedades Hepáticas y Digestivas (CB06/04/1069), Centro de Investigación Biomédica en Red de Enfermedades Cardiovasculares (CB/11/00222), Consorcio de Investigación en Red de la Comunidad de Madrid, S2017/BMD-3686, and Fondo Europeo de Desarrollo Regional. C.L. and M.L.T. are both recipients of FPI fellowships from

MINECO: PRE2021-097824 and PRE2020-094885, respectively. D.F. received a fellowship Ministerio de Educación de Argentina-Fundación Carolina.

CONFLICT OF INTEREST STATEMENT

All authors declare that they have no conflicts of interest.

ORCID

Rocío Brea <https://orcid.org/0000-0003-0517-4045>

Natalia Casanova <https://orcid.org/0000-0002-5632-4886>

Carlota Alvarez-Lucena <https://orcid.org/0000-0002-7115-2111>

Marina Fuertes-Agudo <https://orcid.org/0000-0002-8146-6165>

María Luque-Tevar <https://orcid.org/0000-0003-3074-9197>

Carme Cucarella <https://orcid.org/0000-0002-9501-3861>

María C. Capitani <https://orcid.org/0000-0002-7351-5828>

María V. Marinocchi <https://orcid.org/0000-0002-0140-2330>

Matías E. Fusini <https://orcid.org/0009-0002-2024-7046>

Agustín Lahoz <https://orcid.org/0000-0001-7232-0626>

Marina López Noguerol <https://orcid.org/0000-0003-3114-2231>

Juan Fraile <https://orcid.org/0000-0002-4475-4360>

María T Ronco <https://orcid.org/0000-0002-9503-7089>

Lisardo Bosca  <https://orcid.org/0000-0002-0253-5469>

Águeda González-Rodríguez  <https://orcid.org/0000-0003-2851-2318>

Carmelo García-Monzón  <https://orcid.org/0000-0002-2118-8706>

Paloma Martín-Sanz  <https://orcid.org/0000-0002-0758-9749>

Marta Casado  <https://orcid.org/0000-0001-6457-4650>

Daniel E. Francés  <https://orcid.org/0000-0003-4329-761X>

REFERENCES

- Santamaría E, Rodríguez-Ortigosa CM, Uriarte I, et al. The epidermal growth factor receptor ligand Amphiregulin protects from Cholestatic liver injury and regulates bile acids synthesis. *Hepatology*. 2019;69:1632-1647. doi:10.1002/hep.30348
- Georgiev P, Jochum W, Heinrich S, et al. Characterization of time-related changes after experimental bile duct ligation. *Br J Surg*. 2008;95:646-656. doi:10.1002/BJS.6050
- European Association for the Study of the Liver. EASL clinical practice guidelines: management of cholestatic liver diseases. *J Hepatol*. 2009;51:237-267. doi:10.1016/j.jhep.2009.04.009
- Rodríguez-Garay EA. Cholestasis: human disease and experimental animal models. *Ann Hepatol*. 2003;2:150-158. doi:10.1016/S1665-2681(19)32126-X
- Chiang JYL. Bile acid metabolism and signaling. *Compr Physiol*. 2013;3:1191-1212. doi:10.1002/cphy.c120023
- Guo GL, Chiang JYL. Is CYP2C70 the key to new mouse models to understand bile acids in humans? *J Lipid Res*. 2020;61:269-271. doi:10.1194/JLR.C12000621
- Zhang Y, Hong JY, Rockwell CE, Copple BL, Jaeschke H, Klaassen CD. Effect of bile duct ligation on bile acid composition in mouse serum and liver. *Liver Int*. 2012;32:58-69. doi:10.1111/J.1478-3231.2011.02662.X
- Weng Z, Liu X, Hu J, et al. Protective effect of dehydroandrographolide on obstructive cholestasis in bile duct-ligated mice. *Oncotarget*. 2017;8:87903-87913. doi:10.18632/oncotarget.21233
- Casado M, Mollá B, Roy R, et al. Protection against Fas-induced liver apoptosis in transgenic mice expressing cyclooxygenase 2 in hepatocytes. *Hepatology*. 2007;45:631-638. doi:10.1002/hep.21556
- Francés DE, Ingaramo PI, Mayoral R, et al. Cyclooxygenase-2 overexpression inhibits liver apoptosis induced by hyperglycemia. *J Cell Biochem*. 2013;114:669-680. doi:10.1002/jcb.24409
- Francés DE, Motiño O, Agrá N, et al. Hepatic cyclooxygenase-2 expression protects against diet-induced steatosis, obesity and insulin resistance. *Diabetes*. 2015;64:1522-1531. doi:10.2337/db14-0979
- Motiño O, Agrá N, Brea Contreras R, et al. Cyclooxygenase-2 expression in hepatocytes attenuates non-alcoholic steatohepatitis and liver fibrosis in mice. *Biochim Biophys Acta*. 2016;1862:1710-1723. doi:10.1016/j.bbdis.2016.06.009
- Brea R, Motiño O, Francés D, et al. PGE2 induces apoptosis of hepatic stellate cells and attenuates liver fibrosis in mice by downregulating miR-23a-5p and miR-28a-5p. *Biochim Biophys Acta Mol Basis Dis*. 2018;1864:325-337. doi:10.1016/j.bbdis.2017.11.001
- Motiño O, Francés DE, Casanova N, et al. Protective role of hepatocyte cyclooxygenase-2 expression against liver ischemia-reperfusion injury in mice. *Hepatology*. 2019;70:650-665. doi:10.1002/hep.30241
- Fuertes-Agudo M, Luque-Tévar M, Cucarella C, et al. COX-2 expression in hepatocytes improves mitochondrial function after hepatic ischemia-reperfusion injury. *Antioxidants*. 2022;11:1724. doi:10.3390/antiox11091724
- Kim SM, Park KC, Kim HG, Han SJ. Effect of selective cyclooxygenase-2 inhibitor meloxicam on liver fibrosis in rats with ligated common bile ducts. *Hepatol Res*. 2008;38:800-809. doi:10.1111/j.1872-034X.2008.00339.x
- Chamouard P, Walter P, Baumann R, Poupon R. Prolonged cholestasis associated with short-term use of celecoxib. *Gastroenterol Clin Biol*. 2005;29:1286-1288. doi:10.1016/s0399-8320(05)82223-7
- Ying F, Cai Y, Wong HK, et al. EP4 emerges as a novel regulator of bile acid synthesis and its activation protects against hypercholesterolemia. *Biochimica et Biophysica Acta (BBA) - molecular and cell biology of Lipids*. 2018;1863:1029-1040. doi:10.1016/j.bbalip.2018.06.003
- Cyphert HA, Ge X, Kohan AB, Salati LM, Zhang Y, Hillgartner FB. Activation of the Farnesoid X receptor induces hepatic expression and secretion of fibroblast growth factor 21. *J Biol Chem*. 2012;287:25123-25138. doi:10.1074/jbc.M112.375907
- Yoon J-H, Higuchi H, Werneburg NW, Kaufmann SH, Gores GJ. Bile acids induce cyclooxygenase-2 expression via the epidermal growth factor receptor in a human cholangiocarcinoma cell line. *Gastroenterology*. 2002;122:985-993. doi:10.1053/gast.2002.32410
- Miyaki A, Yang P, Tai H-H, Subbaramaiah K, Dannenberg AJ. Bile acids inhibit NAD⁺-dependent 15-hydroxyprostaglandin dehydrogenase transcription in colonocytes. *Am J Physiol Gastrointest Liver Physiol*. 2009;297:G559-G566. doi:10.1152/ajpgi.00133.2009
- Maillette de Buy Wenniger L, Beuers U. Bile salts and cholestasis. *Dig Liver Dis*. 2010;42:409-418. doi:10.1016/j.dld.2010.03.015
- Kwak BJ, Choi HJ, Kim O-H, et al. The role of Phospho-c-Jun N-terminal kinase expression on hepatocyte necrosis and autophagy in the Cholestatic liver. *J Surg Res*. 2019;241:254-263. doi:10.1016/J.JSS.2019.03.034
- Mayoral R, Mollá B, Flores JM, Bosca L, Casado M, Martín-Sanz P. Constitutive expression of cyclo-oxygenase 2 transgene in hepatocytes protects against liver injury. *Biochem J*. 2008;416:337-346. doi:10.1042/BJ20081224
- Tag C, Weiskirchen S, Hittatiya K, Tacke F, Tolba R, Weiskirchen R. Induction of experimental obstructive cholestasis in mice. *Lab Anim*. 2015;49:70-80. doi:10.1177/0023677214567748
- Ohashi N, Kohn T. Analgesic effect of acetaminophen: a review of known and novel mechanisms of action. *Front Pharmacol*. 2020;11:580289. doi:10.3389/fphar.2020.580289
- Casado M, Callejas NA, Rodrigo J, et al. Contribution of cyclooxygenase 2 to liver regeneration after partial hepatectomy. *FASEB J*. 2001;15:2016-2018. doi:10.1096/fj.01-0158fje
- García-Cañaveras JC, Donato MT, Castell JV, Lahoz A. Targeted profiling of circulating and hepatic bile acids in human, mouse, and rat using a UPLC-MRM-MS-validated method. *J Lipid Res*. 2012;53:2231-2241. doi:10.1194/JLR.D028803
- Motiño O, Francés DE, Mayoral R, et al. Regulation of MicroRNA 183 by cyclooxygenase 2 in liver is DEAD-box helicase p68 (DDX5) dependent: role in insulin signaling. *Mol Cell Biol*. 2015;35:2554-2567. doi:10.1128/MCB.00198-15
- Ahmadi A, Niknahad H, Li H, et al. The inhibition of NFκB signaling and inflammatory response as a strategy for blunting bile acid-induced hepatic and renal toxicity. *Toxicol Lett*. 2021;349:12-29. doi:10.1016/J.TOXLET.2021.05.012
- Huang YH, Yang YL, Huang FC, et al. MicroRNA-29a mitigation of endoplasmic reticulum and autophagy aberrance counteracts in obstructive jaundice-induced fibrosis in mice. *Exp Biol Med*. 2018;243:13-21. doi:10.1177/1535370217741500
- Wang M, Chen M, Zheng G, et al. Transcriptional activation by growth hormone of HNF-6-regulated hepatic genes, a potential mechanism for improved liver repair during biliary injury in mice. *Am J Physiol Gastrointest Liver Physiol*. 2008;295:357-366. doi:10.1152/AJPGI.00581.2007

33. Basiglio CL, Crocenzi FA, Sánchez Pozzi EJ, Roma MG. Oxidative stress and localization status of hepatocellular transporters: impact on bile secretion and role of signaling pathways. *Antioxid Redox Signal*. 2021;35:808-831. doi:[10.1089/ars.2021.0021](https://doi.org/10.1089/ars.2021.0021)
34. Sokol R, Devereaux M, Khandwala R. Effect of dietary lipid and vitamin E on mitochondrial lipid peroxidation and hepatic injury in the bile duct-ligated rat. *J Lipid Res*. 1991;32:1349-1357. doi:[10.1016/S0022-2275\(20\)41965-0](https://doi.org/10.1016/S0022-2275(20)41965-0)
35. Parola M, Leonarduzzi G, Robino G, Albano E, Poli G, Dianzani MU. On the role of lipid peroxidation in the pathogenesis of liver damage induced by long-standing cholestasis. *Free Radic Biol Med*. 1996;20:351-359. doi:[10.1016/0891-5849\(96\)02055-2](https://doi.org/10.1016/0891-5849(96)02055-2)
36. Gu L, Tao X, Xu Y, et al. Dioscin alleviates BDL- and DMN-induced hepatic fibrosis via Sirt1/Nrf2-mediated inhibition of p38 MAPK pathway. *Toxicol Appl Pharmacol*. 2016;292:19-29. doi:[10.1016/J.TAAP.2015.12.024](https://doi.org/10.1016/J.TAAP.2015.12.024)
37. Zhao J, Ran M, Yang T, et al. Bicyclol alleviates signs of BDL-induced cholestasis by regulating bile acids and autophagy-mediated HMGB1/p62/Nrf2 pathway. *Front Pharmacol*. 2021;12:686502. doi:[10.3389/fphar.2021.686502](https://doi.org/10.3389/fphar.2021.686502)
38. Weerachayaphorn J, Mennone A, Soroka CJ, et al. Nuclear factor-E2-related factor 2 is a major determinant of bile acid homeostasis in the liver and intestine. *American journal of physiology-gastrointestinal and liver. Phys Ther*. 2012;302:G925-G936. doi:[10.1152/ajpgi.00263.2011](https://doi.org/10.1152/ajpgi.00263.2011)
39. Park JH, Kwak BJ, Choi HJ, et al. PGC-1 α is downregulated in a mouse model of obstructive cholestasis but not in a model of liver fibrosis. *FEBS Open Bio*. 2021;11:61-74. doi:[10.1002/2211-5463.12961](https://doi.org/10.1002/2211-5463.12961)
40. Miyoshi H, Rust C, Roberts PJ, Burgart LJ, Gores GJ. Hepatocyte apoptosis after bile duct ligation in the mouse involves Fas. *Gastroenterology*. 1999;117:669-677. doi:[10.1016/S0016-5085\(99\)70461-0](https://doi.org/10.1016/S0016-5085(99)70461-0)
41. Leng J, Han C, Demetris AJ, Michalopoulos GK, Wu T. Cyclooxygenase-2 promotes hepatocellular carcinoma cell growth through Akt activation: evidence for Akt inhibition in celecoxib-induced apoptosis. *Hepatology*. 2003;38:756-768. doi:[10.1053/jhep.2003.50380](https://doi.org/10.1053/jhep.2003.50380)
42. Vennemann A, Gerstner A, Kern N, et al. PTGS-2-PTGER2/4 signaling pathway partially protects from diabetogenic toxicity of streptozotocin in mice. *Diabetes*. 2012;61:1879-1887. doi:[10.2337/db11-1396](https://doi.org/10.2337/db11-1396)
43. Straniero S, Laskar A, Savva C, Härdfeldt J, Angelin B, Rudling M. Of mice and men: murine bile acids explain species differences in the regulation of bile acid and cholesterol metabolism. *J Lipid Res*. 2020;61:480-491. doi:[10.1194/JLR.RA119000307](https://doi.org/10.1194/JLR.RA119000307)
44. Tiwari S, Yang J, Morisseau C, Durbin-Johnson B, Hammock BD, Gomes AV. Ibuprofen alters epoxide hydrolase activity and epoxy-oxylipin metabolites associated with different metabolic pathways in murine livers. *Sci Rep*. 2021;11:7042. doi:[10.1038/s41598-021-86284-1](https://doi.org/10.1038/s41598-021-86284-1)
45. Chen K, Li JJ, Li SN, et al. 15-Deoxy- Δ 12,14-prostaglandin J2 alleviates hepatic ischemia-reperfusion injury in mice via inducing antioxidant response and inhibiting apoptosis and autophagy. *Acta Pharmacol Sin*. 2017;38:672-687. doi:[10.1038/aps.2016.108](https://doi.org/10.1038/aps.2016.108)
46. Zhang Y, Desai A, Yang SY, et al. Inhibition of the prostaglandin-degrading enzyme 15-PGDH potentiates tissue regeneration. *Science*. 2015;348:aaa2340. doi:[10.1126/science.aaa2340](https://doi.org/10.1126/science.aaa2340)
47. Núñez O, Fernández-Martínez A, Majano PL, et al. Increased intrahepatic cyclooxygenase 2, matrix metalloproteinase 2, and matrix metalloproteinase 9 expression is associated with progressive liver disease in chronic hepatitis C virus infection: role of viral core and NS5A proteins. *Gut*. 2004;53:1665-1672. doi:[10.1136/gut.2003.038364](https://doi.org/10.1136/gut.2003.038364)
48. Osawa Y, Hannun YA, Proia RL, Brenner DA. Roles of AKT and sphingosine kinase in the antiapoptotic effects of bile duct ligation in mouse liver. *Hepatology*. 2005;42:1320-1328. doi:[10.1002/hep.20967](https://doi.org/10.1002/hep.20967)
49. Georgiev P, Navarini AA, Eloranta JJ, et al. Cholestasis protects the liver from ischaemic injury and post-ischaemic inflammation in the mouse. *Gut*. 2007;56:121-128. doi:[10.1136/gut.2006.097170](https://doi.org/10.1136/gut.2006.097170)
50. Luan X, Chen P, Li Y, et al. TNF- α /IL-1 β -licensed hADSCs alleviate cholestatic liver injury and fibrosis in mice via COX-2/PGE2 pathway. *Stem Cell Res Ther*. 2023;14:100. doi:[10.1186/s13287-023-03342-3](https://doi.org/10.1186/s13287-023-03342-3)

SUPPORTING INFORMATION

Additional supporting information can be found online in the Supporting Information section at the end of this article.

How to cite this article: Brea R, Casanova N, Alvarez-Lucena C, et al. Beneficial effects of hepatic cyclooxygenase-2 expression against cholestatic injury after common bile duct ligation in mice. *Liver Int*. 2024;00:1-15. doi:[10.1111/liv.16004](https://doi.org/10.1111/liv.16004)